Journal of Mechanical Research and Application, JMRA
Vol. 2, No. 1, 2010, 39-45

Nonlinear Deformation Analysis and Modeling of Composite with Aluminum Layers

Habib Esfandiar[1*], Saeed Adib Nazari[2], Vahid Monfared[3], Ali Khatib[4]

Received:10 March 2010; Accepted:15 June 2010

Abstract: Fiber metal laminates (FMLs) are new composite materials consisting of thin metal layers and high strength composite layers. ARALL (Aramid aluminum laminate) is a family of the FML that consists of thin aluminum sheets along with Kevlar/epoxy composite layers. This material has many advantages such as light weight, excellent corrosion, fatigue and impact resistance. Since, ARALL is a new material, therefore presentation of a model for nonlinear behavior analysis is important. This paper presents the elastic– plastic behavior of ARALL under in-plane tensile loading. For this purpose, the orthotropic plasticity theory and modified classical laminated plate theory are used. In the orthotropic plasticity model, a three parameter plastic potential function is used. In the second theory, the Kevlar/epoxy composite layers and aluminum sheets are assumed to be linearly elastic and orthotropic elastic– plastic solids, respectively. Good agreement is obtained between results of two models. The results show that the case study behavior is almost bilinear under tensile loading and it has more strength in longitudinal direction in comparison to transverse direction. Variation of the Poisson's ratio is considered in longitudinal and transverse loading too.

Keywords: Bilinear, FML, Elastic– Plastic, Orthotropic Plasticity, Poisson's Ratio.

1. Introduction

The concept of fiber metal laminates has been developed at Delft University of Technology. In 1979 the first prototype of a fiber metal laminate was tested at this university [1]. This laminate was named ARALL. Currently, FMLs are attracting the interest of a number of aircraft manufacturers. For example, ARALL was used in the manufacture of the cargo door of the American C-17 transport aircraft [2].

ARALL is a new composite material built up from thin aluminum sheets along with high strength Kevlar/ epoxy layers. This material has advantages such as low weight, high corrosion, fatigue and impact resistance and easy machining and forming [3-6]. ARALL also exhibits good stability in corrosion and high temperature [7,8]. The high strength Kevlar fibers improve tensile strength and compression of ARALL material. Since, a multiplicity of metal alloy sheets and basic composite laminate are nowadays accessible, their possible combinations result in a virtually infinite variety of FMLs. Consequently, the selection of the best FML for a given application is a challenging task, requiring reliable tools, capable of predicting how the material response to external stimuli (mechanical stresses, etc.) is correlated with the properties and arrangement of the constituent layers. Wu investigated the in– plane mechanical properties of FML via metal volume fraction approach based on a rule of mixtures [9]. Vogeslang *et al.* presented mechanical properties and features of ARALL [10, 11]. Herakovich presented the Kevlar/ epoxy composite properties based on combination rule [7].

Krishnakumar showed that the tensile strength of many fiber metal laminates is superior to that of traditional aerospace-grade aluminum alloys [2]. Nahas presented several models for nonlinear deformation of FMLs [12]. Often, the laminate constitutive equation has been expressed in incremental form and the problem has been solved by numerical step- by- step iterations, assuming suitable flow rules for plasticity [13-15].

Since, ARALLs consist of aluminum layers and aluminum has nonlinear behavior, therefore elastic analysis is not sufficient and hence a model for exact prediction of nonlinear tensile response must be presented. To achieve such model, Kevlar/epoxy composite should be modeled as an orthotropic

1*. Corresponding Author: M. Sc., Islamic Azad University, Firozkouh Branch, Firozkouh, Iran (habib_esfandiar_2006@yahoo.com)
2. Associate Professor, Islamic Azad University, Research and Science Branch, Tehran, Iran (adib@sharif.edu)
3. M. Sc., Islamic Azad University, Zanjan Branch, Zanjan, Iran (vahid_monfared@alum.sharif.edu)
4. M. Sc., Islamic Azad University, Khomeinishahr Branch, Khomeinishahr, Iran (khatib@iaukhsh.ac.ir)

linearly elastic solid and aluminum is assumed as an elasto- plastic solid.

In this paper, the nonlinear tensile response of ARALL laminate is investigated under static tensile loading condition. Two approaches as orthotropic plasticity and modified laminated plate theories are used to predict the stress–strain response and deformation behavior of ARALL laminate. The stress–strain relation and Poisson's ratio response of ARALL laminate under static tensile loading are also analyzed.

2. Mechanical description

In this study, the ARALL 3/2, consists of three layers of 2024- T4 aluminum alloy sheets and two layers of Kevlar/epoxy composite with fibers in the $0^\circ/90^\circ/0^\circ$ orientation, is used (Figs. 1 and 2). The 2024– T4 aluminum alloy and Kevlar/epoxy are modeled as elasto – plastic and orthotropic linearly elastic solids, respectively. Mechanical properties of aluminum alloy and Kevlar/ epoxy have been presented in table 1.

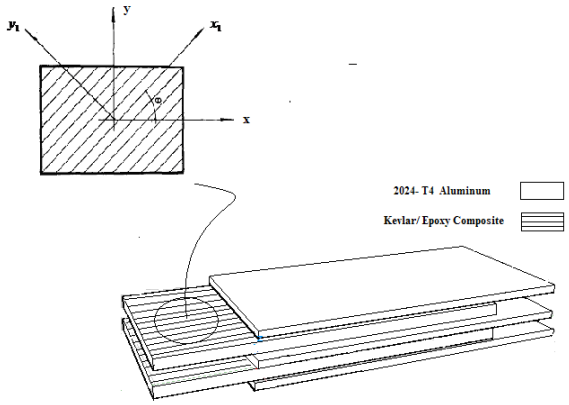

Fig. 1. The ARALL laminate and definition coordinate for composite

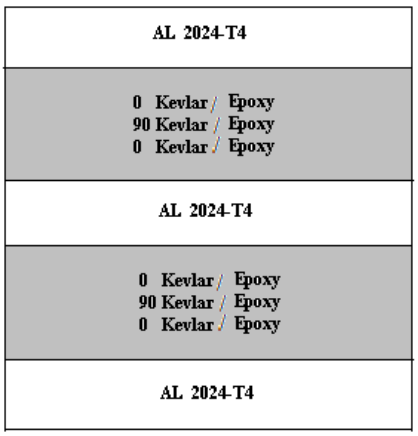

Fig. 2. The schematic view of ARALL 3/2 and fiber directions

3. An orthotropic plasticity model

The first approach for reaching to nonlinear response of ARALL is an orthotropic plasticity model. For analyzing ARALL 3/2, in– plane plastic potential function with three parameters has been used [14].

$$f(\sigma_{ij}) = \frac{1}{2}\left[a_{11}\sigma_{11}^2 + \sigma_{22}^2 + 2a_{12}\sigma_{11}\sigma_{22} + 2a_{66}\sigma_{12}^2\right] \quad (1)$$

For elasto– plastic response of aluminum the flow rule is used as follows:

$$d\varepsilon_{ij}^p = d\lambda \frac{\partial f}{\partial \sigma_{ij}} \quad (2)$$

Where $d\lambda$ is proportional factor. From Eqs. (1) and (2), plastic strain increment is presented to matrix form as:

$$\begin{Bmatrix} d\varepsilon_{11}^p \\ d\varepsilon_{22}^p \\ d\varepsilon_{12}^p \end{Bmatrix} = \begin{bmatrix} a_{11} & a_{12} & 0 \\ a_{12} & 1 & 0 \\ 0 & 0 & 2a_{66} \end{bmatrix} \begin{Bmatrix} \sigma_{11} \\ \sigma_{22} \\ \sigma_{12} \end{Bmatrix} d\lambda \quad (3)$$

Where subscripts 1 and 2 indicate the fiber and transverse directions, respectively.

By defining the effective stress as [14]:

$$\bar{\sigma} = \sqrt{3f} \quad (4)$$

And the effective plastic strain increment as [14]:

$$d\bar{\varepsilon}^p = \left(\frac{2}{3(a_{11}-a_{12})}\right)^{1/2} \left(\begin{array}{l} \left(d\varepsilon_{11}^p\right)^2 + a_{11}\left(d\varepsilon_{22}^p\right)^2 - 2a_{12}d\varepsilon_{11}^p d\varepsilon_{22}^p \\ + \dfrac{\left(a_{11}-a_{12}^2\right)}{2a_{66}}\left(d\varepsilon_{12}^p\right)^2 \end{array}\right)^{1/2} \quad (5)$$

Thus, plastic work increment can be written as:

$$dW^p = \sigma_{ij}d\varepsilon_{ij}^p = \bar{\sigma}d\bar{\varepsilon}^p = 2fd\lambda \quad (6)$$

Therefore, $d\lambda$ is derived as:

$$d\lambda = \frac{3d\bar{\varepsilon}^p}{2\bar{\sigma}} = \frac{3}{2}\left(\frac{d\bar{\varepsilon}^p}{d\bar{\sigma}}\right)\left(\frac{d\bar{\sigma}}{\bar{\sigma}}\right) \quad (7)$$

Table 1. Mechanical properties of ARALL

Material	E_{11}(GPa)	E_{22} (GPa)	ν_{12}	G_{12} (GPa)
Aluminum 2024- T4	73	73	0.33	26.6
Kevlar/epoxy composite	61.38	4.14	0.425	1.38

E= Elastic modulus, v= Poisson's ratio, G= Shear modulus

To complete the stress-strain incremental plastic relation, the relation between the effective stress and effective plastic strain should be estimated. Thus, the power law should be used as [14]:

$$\bar{\varepsilon}^p = \beta(\bar{\sigma})^\gamma \tag{8}$$

By considering the $x-y$ and x_1-y_1 coordinates (see Fig. 1) and uniaxial stress in x direction and using rotational matrix T in Eq. (9), the principle stresses are:

$$T=\begin{bmatrix} \cos^2\theta & \sin^2\theta & -2\sin\theta\cos\theta \\ \sin^2\theta & \cos^2\theta & -2\sin\theta\cos\theta \\ -\sin\theta\cos\theta & \sin\theta\cos\theta & \cos^2\theta-\sin^2\theta \end{bmatrix} \tag{9}$$

$$\begin{Bmatrix}\sigma_{11}\\ \sigma_{22}\\ \sigma_{12}\end{Bmatrix}=[T]\begin{Bmatrix}\sigma_x\\ 0\\ 0\end{Bmatrix}$$

$$\sigma_{11}=\sigma_x\cos^2\theta$$

$$\sigma_{22}=\sigma_x\sin^2\theta \tag{10}$$

$$\sigma_{12}=-\sigma_x\sin\theta\cos\theta$$

Using the introduced rotational matrix for strains and Eqs. (1) -(5), gives:

$$\bar{\sigma}=g(\theta)\,\sigma_x \qquad d\bar{\varepsilon}^p=\frac{d\varepsilon_x^p}{g(\theta)} \tag{11}$$

Where ε_x^p denotes plastic strain in x direction and $g(\theta)$ is [14]:

$$g(\theta)=\sqrt{\frac{3}{2}}(a_{11}\cos^4\theta+\sin^4\theta + 2(a_{12}+a_{66})\sin^2\theta\cos^2\theta)^{1/2} \tag{12}$$

Thus, the desired relation between $\bar{\varepsilon}^p-\bar{\sigma}$ can be obtained from the ε^p,σ_x and Eq. (12). Now, a_{66},a_{12},a_{11} parameters selection is single problem to achieve $\bar{\varepsilon}^p-\bar{\sigma}$ relation. Plastic Poisson's ratio definition is one way for the selection of these parameters. Using Eqs. (3) and (10) and the coordinate transformation on strain components, the plastic strain increments in the x direction and y direction can be obtained as:

$$\begin{aligned} d\varepsilon_x^p &= d\lambda\sigma_x(a_{11}\cos^4\theta+\sin^4\theta \\ &\quad +2(a_{12}+a_{66})\sin^2\theta\cos^2\theta) \\ d\varepsilon_y^p &= d\lambda\sigma_x((1+a_{11}-2a_{66})\sin^2\theta\cos^2\theta \\ &\quad +a_{12}(\sin^4\theta+\cos^4\theta)) \end{aligned} \tag{13}$$

Thus, the plastic Poisson's ratio is:

$$\nu^p=-\frac{d\varepsilon_y^p}{d\varepsilon_x^p}$$

$$=-\frac{(1+a_{11}-2a_{66})\sin^2\theta\cos^2\theta+}{a_{11}\cos^4\theta+\sin^4\theta+}$$

$$\frac{a_{12}(\sin^4\theta+\cos^4\theta)}{2(a_{12}+a_{66})\sin^2\theta\cos^2\theta}$$

Using above equations and Poisson's ration in $\theta=0^\circ,90^\circ,45^\circ$, the plastic Poisson's ratios are:

$$\nu^p(\theta=0)=-\frac{a_{12}}{a_{11}}\ ,\ \nu^p(\theta=90)=-a_{12}\ ,\ \nu^p(\theta=45)=-\frac{1+a_{11}+2(a_{12}-a_{66})}{1+a_{11}+2(a_{12}+a_{66})} \tag{15}$$

To simplifying, give:

$$a_{11}=\frac{\nu^p(\theta=90)}{\nu^p(\theta=0)}$$

$$a_{12}=-\nu^p(\theta=90)$$

$$a_{66}=-\frac{1+\left[\nu^p(\theta=90)\big/\nu^p(\theta=0)\right]-2\nu^p(\theta=90)}{2}=-\frac{1+a_{11}+2a_{12}}{2} \tag{16}$$

4. Analytical prediction by modified laminated plate theory

An analytical model incorporating the elasto-plastic behavior of aluminum sheets of ARALL is used to determine the stress-strain relation of ARALL. The most important assumptions that should be considered for the analysis of ARALL with this theory are as follows:

a. The composite fibers in any layer are parallel.

b. Distance between fibers in any layer is equal.

c. All fibers in all layers are continues and have same cross section.

d. Fibers are in perfect bonding to matrix.

For a general orthotropic laminate subjected to in– plane loading, strain vary linear in thickness direction but stress vary just linear in thickness direction in any layer. Therefore, an equivalent force– moment system replacing stress is used as

follows [16]:

$$\begin{Bmatrix} N \\ M \end{Bmatrix} = \begin{bmatrix} A & B \\ B & D \end{bmatrix} \begin{Bmatrix} \varepsilon^{\circ} \\ k \end{Bmatrix} \tag{17}$$

Where N and M denote the in – plane force and moment per unit length and ε°, k indicate the mid - plane strains and curvature, respectively. *A, B and D* matrices are extensional stiffness matrix, coupling stiffness matrix and bending stiffness matrix, respectively. *A, B and D* matrices are calculated as [16]:

$$[A,B,D] = \int_{-h/2}^{h/2} [Q]\left(1, z, z^2\right) dz \tag{18}$$

Where h and $[Q]$ are laminate thickness and reduced stiffness matrix, respectively.

ARALL 3/2 is orthotropic and symmetrical with respect to the mid– plane. Thus, matrix B and (2,6), (1,6) elements of matrix D are zero. Therefore, the resultant forces and moments are obtained as:

$$[\mathrm{N},\mathrm{M}] = \int_{-h/2}^{h/2} [\sigma]^{\mathrm{i}}(1,\mathrm{z})\, \mathrm{dz}$$

$$\begin{bmatrix} \sigma_{11} \\ \sigma_{22} \\ \sigma_{12} \end{bmatrix}^{\mathrm{i}} = \begin{bmatrix} \mathrm{Q}_{11} & \mathrm{Q}_{12} & 0 \\ \mathrm{Q}_{12} & \mathrm{Q}_{22} & 0 \\ 0 & 0 & \mathrm{Q}_{66} \end{bmatrix}^{\mathrm{i}} \left(\begin{bmatrix} \varepsilon^{\circ}_{11} \\ \varepsilon^{\circ}_{22} \\ \varepsilon^{\circ}_{12} \end{bmatrix} + \mathrm{z} \begin{bmatrix} \mathrm{k}_{11} \\ \mathrm{k}_{22} \\ \mathrm{k}_{12} \end{bmatrix} \right)^{\mathrm{i}} \tag{19}$$

Where $[\sigma]^i$ is stress in i th ply at a distance z. Due to compatibility of the layers in ARALL laminate, all layers experience same deformation such that [7]:

$$\{\varepsilon^{AR}\} = \{\varepsilon^{C}\} = \{\varepsilon^{AL}\} \tag{20}$$

Where $\{\varepsilon^{AR}\}$ denotes the ARALL strain vector.

Under a uniaxial in– plane tensile load, the deformation response of the laminate is described by the following relation [17]:

$$dN = [A][d\varepsilon] \tag{21}$$

Where dN is increments of the in- plane force per unit length and can be expressed as:

$$dN = h[d\sigma] \tag{22}$$

The reduced stiffness matrix A is calculated as:

$$[A] = n_{AL} h_{AL} [Q]_{AL} + n_C h_C [Q]_C \tag{23}$$

Where h_{AL}, n_{AL} are thickness and number of aluminum sheets, respectively and h_C, n_C denote thickness and number of Kevlar/ epoxy composite layers, respectively.

4.1. Kevlar/epoxy composite model

The Kevlar/ epoxy lamina is assumed to be a linear orthotropic elastic solid and the incremental stress- strain relation is [7]:

$$\begin{aligned} &[d\sigma^C] = [Q]_C [d\varepsilon^C] \\ &[d\sigma^C] = \{d\sigma^C{}_{11}\ d\sigma^C{}_{22}\ \ d\sigma^C{}_{12}\}^T \\ &[d\varepsilon^C] = \{d\varepsilon^C{}_{11}\ \ d\varepsilon^C{}_{22}\ \ d\varepsilon^C{}_{12}\}^T \end{aligned} \tag{24}$$

Where $[Q]_C$ is Kevlar/ epoxy composite stiffness matrix and is:

$$[Q]_C = \begin{bmatrix} \frac{E_{11}}{L} & \frac{-\nu_{12}E_{22}}{L} & 0 \\ \frac{-\nu_{12}E_{22}}{L} & \frac{E_{22}}{L} & 0 \\ 0 & 0 & G_{12} \end{bmatrix}^C, \tag{25}$$

$$L = 1 - \nu_{12}{}^C \nu_{21}{}^C$$

The Kevlar/epoxy composite properties were presented in table 1.

4.2. Constitutive model for 2024 - T4 aluminum

In this study, the 2024-T4 aluminum is modeled to be orthotropic elasto– plastic solid similar to that described in section (2). Thus, it is necessary that 2024–T4 aluminum alloy is modeled to two parts such that first part denotes elastic deformation and second part describes plastic deformation behavior. For the elastic part of the aluminum deformation, give [7]:

$$\left[d\varepsilon^{AL}\right]^{EL} = \left[S^{AL}\right]_{EL} \left[d\sigma^{AL}\right]^{EL} \tag{26}$$

Where $\left[S^{AL}\right]_{EL}$ is aluminum alloy flexibility matrix for elastic deformation and is:

$$\left[S^{AL}\right]_{EL} = \begin{bmatrix} \frac{1}{E} & \frac{-\nu}{E} & 0 \\ \frac{-\nu}{E} & \frac{1}{E} & 0 \\ 0 & 0 & \frac{1}{G} \end{bmatrix}^{AL} \tag{27}$$

Where AL, EL symbols denote elastic properties of the aluminum that were given in table 2.

For the plastic deformation of the aluminum, the plastic potential is taken as [7]:

$$f^{AL}(\sigma_{ij}) = \frac{1}{2}[a_{11}\left(\sigma_{11}^{AL}\right)^2 + \left(\sigma_{22}^{AL}\right)^2 - \sigma_{11}^{AL}\sigma_{22}^{AL} + 3\left(\sigma_{12}^{AL}\right)^2] \tag{28}$$

Table 2. Geometrical properties and volume fraction of the ARALL 3/2

Material	Thickness (mm)	Length (mm)	Width (mm)	Volume Fraction
Aluminum 2024-T4	0.305	255	25.5	0.68
Kevlar/ Epoxy Composite	0.45	255	25.5	0.32

Where a_{11} parameter denotes difference between the plastic portions of longitudinal and transverse directions.

Note that Eq. (28) is special case of Eq. (1) when $a_{66}=\frac{3}{2}$, $a_{12}=\frac{-1}{2}$ and can be reduced to the Von-Mises function when $a_{11}=1$.

In this paper, a power law to showing the relationship between effective stress and effective plastic strain is used as follows:

$$\bar{\varepsilon}_P^{AL}=\beta^{AL}\left(\bar{\sigma}^{AL}\right)^{\gamma} \tag{29}$$

Thus,

$$\begin{aligned} d\lambda_{AL}&=\frac{3d\bar{\varepsilon}_P^{AL}}{2\bar{\sigma}^{AL}}\\ &=\Omega\left[\psi_1 d\sigma_{11}^{AL}+\psi_2 d\sigma_{22}^{AL}+\psi_3 d\sigma_{12}^{AL}\right] \end{aligned} \tag{30}$$

Where

$$\begin{aligned} \Omega&=\frac{9}{4}\beta_{AL}\gamma\left(\bar{\sigma}^{AL}\right)^{\gamma-3}\\ \psi_1&=\frac{1}{2}\left(2a_{11}\sigma_{11}^{AL}-\sigma_{22}^{AL}\right)\\ \psi_2&=\frac{1}{2}\left(2\sigma_{22}^{AL}-\sigma_{11}^{AL}\right)\\ \psi_3&=3\sigma_{12}^{AL} \end{aligned} \tag{31}$$

The relation between plastic strain increment and the stress increment are taken as:

$$\left[d\varepsilon^{AL}\right]^P=\left[S^{AL}\right]_P\left[d\sigma^{AL}\right]^P \tag{32}$$

Where $\left[S^{AL}\right]_P$ is aluminum alloy flexibility matrix for plastic deformation and is:

$$\left[S^{AL}\right]_P=\begin{bmatrix}\Omega\psi_1\psi_1 & \Omega\psi_1\psi_2 & \Omega\psi_1\psi_3\\ \Omega\psi_1\psi_2 & \Omega\psi_2\psi_2 & \Omega\psi_2\psi_3\\ \Omega\psi_1\psi_3 & \Omega\psi_2\psi_3 & \Omega\psi_3\psi_3\end{bmatrix}^{AL}_P \tag{33}$$

Therefore, stress-strain relation for the aluminum is:

$$\begin{aligned} \left[d\varepsilon^{AL}\right]&=\left[S^{AL}\right]\left[d\sigma^{AL}\right],\\ \left[S^{AL}\right]&=\left[S^{AL}\right]_{EL}+\left[S^{AL}\right]_P \end{aligned} \tag{34}$$

$$\begin{aligned} \left[d\sigma^{AL}\right]&=\left[Q^{AL}\right]\left[d\varepsilon^{AL}\right],\\ \left[Q^{AL}\right]&=\left[S^{AL}\right]^{-1} \end{aligned}$$

5. Results and discussion

In order to illustrate the behavior of the ARALL 3/2 under longitudinal and transverse loading, the following section is presented.

5.1. Result of orthotropic plasticity model

By considering the orthotropic plasticity model for the ARALL laminate, then all of longitudinal stress- strain curves should reduced into a single curve versus effective stress and effective plastic strain. This is the basis for determining the values of a_{11}, a_{12} and a_{66} parameters in the plastic potential function. From Eq. (12) can be found that $g(90)=\sqrt{\frac{3}{2}}$ and is independent of a_{11}, a_{12} and a_{66} parameters. Using the stress- strain curve of the $\theta=90^\circ$, give:

$$\beta=55.2,\ \gamma=8.05 \tag{35}$$

For values of parameters a_{11} and $a_{12}+a_{66}$ in $g(\theta)$ should make the effective stress and effective plastic strain curves fall on the stress-strain curve for $\theta=90^\circ$.

Thus, a reasonable set of values of introduced parameters is:

$$a_{11}=0.36,\ a_{12}+a_{66}=1.3 \tag{36}$$

The stress-strain relation for ARALL 3/2 in both the longitudinal and transverse directions has been shown in Fig. 3.

5.2. Results of modified laminated plate model

As mentioned before in section (4), the values of parameters a_{11}, γ and β_{AL} are necessary for using laminated plate model. Thus, for fibers orientation $\theta=0^\circ,\ 90^\circ$ may be written as:

$$g(90)=\sqrt{\frac{3}{2}},\quad g(0)=\sqrt{\frac{3}{2}}a_{11} \tag{37}$$

Where effective stress and effective plastic strain relations are independent of parameter a_{11} in $\theta=90^\circ$.

This note can be used to calculate parameters γ. and β_{AL} by least square method, parameters γ, β_{AL} and a_{11} are:

$$\beta_{AL}=0.478\times10^4,\quad \gamma=15,\quad a_{11}=0.787 \tag{38}$$

Using above values for parameters γ, β_{AL} and a_{11} and under uniaxial loading condition, the stress-strain curve is shown in Fig. 4.

Fig. 3 and 4 show the tensile stress-strain relation for ARALL 3/2 in both the longitudinal and transverse directions. From figures can be found that ARALL 3/2 vary almost linear in plastic part similar to elastic region in the longitudinal loading. In the transverse loading, a similar stress-strain response to the longitudinal direction is gained. These mean that ARALL 3/2 exhibits a bilinear stress-strain behavior in the both longitudinal and transverse directions. Of course, the stress-strain response specifications such as yield stress, hardening modulus and tensile fracture stress in the transverse loading are lower than longitudinal direction due to $0^\circ, 90^\circ, 0^\circ$ orientation of fibers. It can be seen that ARALL 3/2 has two different slopes in elastic and plastic parts (unequal elastic modulus and hardening modulus).

Fig. 5 shows the Poisson's ratio response (ratio of transverse and axial strains) of ARALL 3/2 for both the longitudinal and transverse directions. It can be seen that Poisson's ratio response in the transverse loading is lower than the similar case in longitudinal loading such that difference between longitudinal and transverse loadings will be increased by increasing the value of axial strain. This fact is due to $0^\circ, 90^\circ, 0^\circ$ orientation of fibers as described above. Extracted results from two models, orthotropic plasticity and modified laminated plate models, have good agreement (see Figs. 3 and 4).

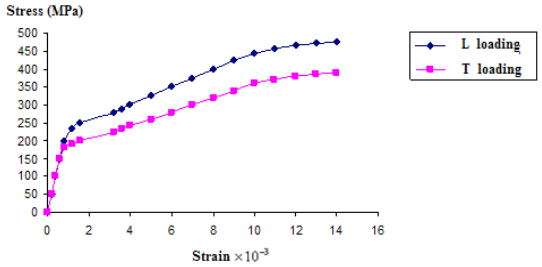

Fig. 3. Stress-strain curve of ARALL 3/2 in longitudinal (L) and transverse (T) directions from orthotropic plasticity model

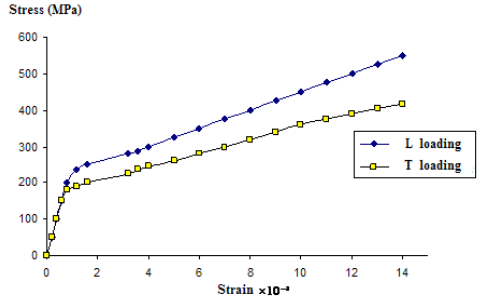

Fig. 4. Stress-strain curve of ARALL 3/2 in longitudinal (L) and transverse (T) directions from modified laminated plate model

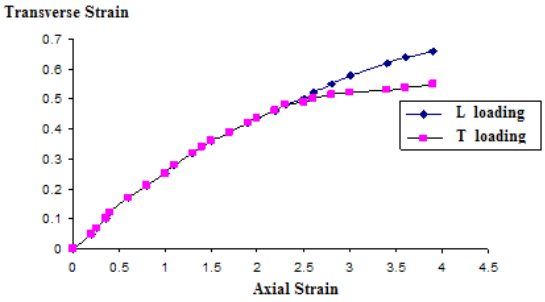

Fig. 5. The Poisson's ratio response in longitudinal (L) and transverse (T) directions for ARALL 3/2

6. Conclusions

In this paper the elasto– plastic behavior of ARALL 3/2 under in– plane tensile loading via two approaches as orthotropic plasticity and modified laminated plate theories has been investigated. Aluminum layers in ARALL have been modeled as orthotropic elasto- plastic solids and Kevlar/epoxy composite layers have been considered as orthotropic linearly elastic solids. Results showed that ARALL 3/2 is stronger than aluminum alloy and stress- strain response is almost bilinear in both fibers and transverse directions. From stress-strain curves it was found that ARALL 3/2 has more strength in longitudinal direction in comparison to transverse direction. Analytical predictions by modified laminated plate theory showed good agreement with results of orthotropic plasticity model. It has been notice that Poisson's ratio response in the transverse loading is lower than similar case in longitudinal loading due to $0^\circ, 90^\circ, 0^\circ$ orientation of fibers.

References

[1] Vlot, A., "Glare history of the development of a new aircraft material, Dordrecht", The Netherlands: Kluwer Academic Publishers, 2001.

[2] Krishnakumar, S., "Fiber metal laminates - the synthesis of metals and composites", Mater. Manuf. Processes, 1995, 9, 295–354.

[3] Marissen, R., "Flight simulation behavior of Aramid reinforced aluminum laminates", Engineering Fracture Mechanics, 1984, 19, 261- 77.

[4] Vermeeren, C., "An historic overview of the development of fiber metal laminates", Appl. Compos. Mate., 2003, 10, 189.

[5] Kawai, M.; Morishita, M.; Tomura, S.; Takumida, K., "Inelastic behavior and strength of fiber–metal hybrid composite: GLARE", Int J M ech Sci, 1998, 40, 183–198.

[6] Sinke, J., "Manufacturing of GLARE parts and structures", Appl. Compos. Mater., 2003, 10, 293-305.

[7] Herakovich, C. T., "Mechanical and thermal characterization of unidirectional Aramid/ Epoxy", Presented at ARALL Laminates Technical Confrrence, Pennsylvania, 25-28 October, 1987.

[8] Wu, G.; Yang, J. M., "The mechanical behavior of GLARE laminates for aircraft structures", J. Miner. Met. Mater. Soc., 2005, 9, 57-72.

[9] Wu, H. F.; Wu, L. L., "Use of rule of mixtures and metal volume fraction for mechanical property predictions of fiber-reinforced aluminum laminates", J. Mater. Sci., 1994, 29, 45-83.

[10] Vogeslang, L. B.; Vlot, A., "Development of fiber metal laminates for advanced aerospace materials", J. Mater. Process. Technol., 1, 2000, 103.

[11] Hagenbeek, M.; Van Hengel C.; Bosker O. J.; Vermeeren CAJR, Static properties of fiber metal laminates, Appl. Compos. Mater., 2003, 10, 297.

[12] Nahas, M. N., "Analysis of non-linear stress–strain response of laminated fiber-reinforced composites Fiber", Sci. Technol., 1984, 20, 297.

[13] Hidde, J. S.; Herakovich, C. T., "Inelastic response of hybrid composite laminates", J. of Compos. Mater., 1992, 26, 2-19.

[14] Kenaga, D.; Doyle, J. F., "The characterization of boron/aluminum composite in nonlinear range as an orthotropic elastic- plastic material", J. of Compos. Mater., 1987, 21, 516-531.

[15] Petit, P. H.; Waddoups, M. E., "A method of predicting the nonlinear behavior of laminated composites", J. of Compos. Mater., 1969, 3, 2-19.

[16] Jones, R. M., "Mechanics of composite materials", 2nd ed, Philadelphia: Taylor and Francis, 1998.

[17] Mallick, P. K., "Fiber- reinforced composites; materials, manufacturing and design", New York: Dekker, 1988.